THE JOURNAL OF BIOLOGICAL CHEMISTRY VOL. 282, NO. 42, pp. 30570–30576, October 19, 2007

A Novel N-terminal Isoform of the Neuron-specific K-Cl Cotransporter KCC2*[S]

Received for publication, June 21, 2007, and in revised form, August 20, 2007 Published, JBC Papers in Press, August 22, 2007, DOI 10.1074/jbc.M705095200

Pavel Uvarov[‡1,2], Anastasia Ludwig[§1], Marika Markkanen[‡], Priit Pruunsild[¶], Kai Kaila[‡‖], Eric Delpire[**], Tõnis Timmusk[¶], Claudio Rivera[§], and Matti S. Airaksinen[‡3]

From the [‡]Neuroscience Center, Viikinkaari 4, [§]Institute of Biotechnology, Viikinkaari 9, and [‖]Department of Biological and Environmental Sciences, Viikinkaari 1, University of Helsinki, 00014 Helsinki, Finland, the [¶]Department of Gene Technology, Tallinn University of Technology, Akadeemia tee 15, Tallinn 19086, Estonia, and the [**]Department of Anesthesiology, Vanderbilt University Medical Center, Nashville, Tennessee 37232

The neuronal K-Cl cotransporter KCC2 maintains the low intracellular chloride concentration required for the hyperpolarizing actions of inhibitory neurotransmitters γ-aminobutyric acid and glycine in the central nervous system. This study shows that the mammalian KCC2 gene (alias Slc12a5) generates two neuron-specific isoforms by using alternative promoters and first exons. The novel KCC2a isoform differs from the only previously known KCC2 isoform (now termed KCC2b) by 40 unique N-terminal amino acid residues, including a putative Ste20-related proline alanine-rich kinase-binding site. Ribonuclease protection and quantitative PCR assays indicated that KCC2a contributes 20–50% of total KCC2 mRNA expression in the neonatal mouse brain stem and spinal cord. In contrast to the marked increase in KCC2b mRNA levels in the cortex during postnatal development, the overall expression of KCC2a remains relatively constant and makes up only 5–10% of total KCC2 mRNA in the mature cortex. A rubidium uptake assay in human embryonic kidney 293 cells showed that the KCC2a isoform mediates furosemide-sensitive ion transport activity comparable with that of KCC2b. Mice that lack both KCC2 isoforms die at birth due to severe motor defects, including disrupted respiratory rhythm, whereas mice with a targeted disruption of the first exon of KCC2b survive for up to 2 weeks but eventually die due to spontaneous seizures. We show that these mice lack KCC2b but retain KCC2a mRNA. Thus, distinct populations of neurons show a differential dependence on the expression of the two isoforms: KCC2a expression in the absence of KCC2b is presumably sufficient to support vital neuronal functions in the brain stem and spinal cord but not in the cortex.

The neuron-specific K-Cl cotransporter KCC2 maintains the low intracellular chloride concentration that is necessary for the hyperpolarizing actions of inhibitory neurotransmitters γ-aminobutyric acid and glycine in mature central nervous system (CNS)[4] neurons (1–4). During embryonic development, KCC2 mRNA expression follows neuronal maturation, first becoming detectable in the postmitotic neurons of the brain stem and spinal cord and then gradually increasing in higher brain structures (5–7).

The use of alternative promoters, and consequently alternative first exons, is thought to play a pivotal role in generating the complexity required for highly elaborated molecular systems in brain development. More than 50% of human genes may be regulated by alternative promoters, resulting in a wide variety of transcripts (8). Alternative transcripts may have different expression patterns and can be translated into proteins with different structures, phosphorylation patterns, or subcellular localizations, thus providing a molecular mechanism for the fine-tuning of gene functions (9). Indeed, alternative splice forms of K-Cl cotransporters KCC1 and KCC3 with different expression patterns (10–12) and regulation (13) have been described, although their physiological role remains mostly unclear.

Here we describe a novel KCC2 isoform (hereby named KCC2a) that differs from the previously characterized KCC2 isoform (now termed KCC2b) by 40 amino acids in the N terminus encoded by an alternatively spliced exon (named exon-1a). Like KCC2b, the expression of KCC2a mRNA is restricted to CNS neurons. KCC2a contributes 20–50% of the total KCC2 mRNA expression in the neonatal mouse brain stem and spinal cord but only 5–10% in the mature cortex. We also show that mice with a targeted disruption of KCC2 exon-1b (14) lack KCC2b but retain KCC2a mRNA. Because these mice survive for 2 weeks (14), whereas mice that lack both KCC2 isoforms die at birth due to severe motor defects (3), KCC2a is presumably important for the basic neuronal network functions in the brain stem and spinal cord required for survival.

* This work was supported by grants from the Academy of Finland, the University of Helsinki, and the Sigrid Jusélius Foundation (to M. S. A. and C. R.) and by Wellcome Trust, the Estonian Science Foundation, and the Estonian Ministry of Education and Research (to T. T.). The costs of publication of this article were defrayed in part by the payment of page charges. This article must therefore be hereby marked "*advertisement*" in accordance with 18 U.S.C. Section 1734 solely to indicate this fact.

The nucleotide sequence(s) reported in this paper has been submitted to the DDBJ/GenBank™/EBI Data Bank with accession number(s) EF641113.

[S] The on-line version of this article (available at http://www.jbc.org) contains supplemental Figs. S1–S3 and supplemental Table S1.

[1] Both authors contributed equally to this work.

[2] To whom correspondence may be addressed. E-mail: pavel.uvarov@helsinki.fi.

[3] To whom correspondence may be addressed. E-mail: matti.airaksinen@helsinki.fi.

[4] The abbreviations used are: CNS, central nervous system; RACE, rapid amplification of cDNA ends; RPA, ribonuclease protection assay; RT-PCR, reverse transcription PCR; GAPDH, glyceraldehyde-3-phosphate dehydrogenase; HEK, human embryonic kidney; NEM, *N*-ethylmaleimide; UTR, untranslated region; SPAK, Ste20-related proline alanine-rich kinase; OSR1, oxidative stress response 1; Rb, rubidium.

EXPERIMENTAL PROCEDURES

Sequence Analysis—CpG islands inside the KCC2 gene were analyzed using the CpGPlot tool. The expressed sequence tag data base (dbEST) was BLAST-searched using the upstream CpG island I sequence (~400 bp) as a query, and the hits obtained were analyzed against the genome data base. Phosphorylation patterns were predicted with Scansite (15). Sequences of primers used in this study appear in supplemental Table S1.

Rapid Amplification of cDNA Ends (RACE)—5′-RACE was performed using the mouse 15-day embryo Marathon-ready cDNA kit (BD Biosciences Clontech, Mountain View, CA). The first round of amplification was performed with adapter primer AP1 from the kit and KCC2 exon-1a-specific reverse R1a primer (supplemental Table S1). An aliquot from the first reaction was used for nested PCR with adapter primer AP2 from the kit and KCC2 exon-1a-specific reverse R1a-2 primer. The PCR conditions were: 2 min at 95 °C followed by 40 cycles (first round) or 30 cycles (second round) at 95 °C for 30 s, 60 °C for 30 s, and 72 °C for 60 s. Products were analyzed on 1.5% agarose gel, purified with the QIAquick gel extraction kit (Qiagen), ligated into the pGEM-T Easy vector (Promega, Madison, WI), and sequenced. The results were confirmed with another RACE kit (GeneRacer; Invitrogen) using RNA prepared from adult mouse brain (data not shown).

Ribonuclease Protection Assay (RPA)—RPA was performed as described previously (16) using the RPA kit from Ambion (Austin, TX). RNA was isolated using RNAwiz (Ambion). A 195-bp PCR fragment, comprising 27 bp of exon-1a, 95 bp of exon-2, and 73 bp of exon-3 of the mouse KCC2 gene was amplified with primers F1a and R3 (supplemental Table S1), ligated into the pGEM-T Easy vector, and sequenced. To generate a ^{32}P-labeled antisense RNA probe, the vector was linearized at a unique AvaI restriction site in KCC2 exon-1a. Thus, the length of the protected fragment corresponding to KCC2a mRNA was 186 bp *versus* 168 bp for the KCC2b isoform.

Quantitative RT-PCR Analysis—Total RNA was isolated with RNeasy Micro (Qiagen) or NucleoSpin RNA II (Macherey-Nagel, Düren, Germany) kits. Typically, ~1 μg of total RNA was reverse-transcribed using SuperScript III Reverse Transcriptase (Invitrogen) and either random or KCC2 exon-2-specific primers (at 37 or 55 °C, respectively) according to the manufacturer's protocol. The cDNA samples were amplified using the DyNAmo Flash SYBR Green quantitative PCR kit (Finnzymes) and detected via the ABI Prism 7000 Sequence Detection System (Applied Biosystems). Primers for KCC2a, KCC2b, and glyceraldehyde-3-phosphate dehydrogenase (GAPDH) quantification were designed with Express v2.0 software (Applied Biosystems) or manually and contained an intronic sequence in between (supplemental Table S1).

Expression Constructs—To obtain KCC2a and KCC2b expression constructs with an identical backbone, we prepared the full-length KCC2a cDNA by substituting the nucleotides corresponding to exon-1b with exon-1a in the full-length KCC2b cDNA. For this, a 5′-fragment of rat KCC2a cDNA was first amplified by PCR using primers specific for exon-1a (F1a-3) and exon-7 (R7) (supplemental Table S1) and subcloned into the pGEM-T Easy vector. This was then digested with SpeI (in the polylinker) and MunI (in exon-5 of KCC2) and ligated into a vector carrying the full-length rat KCC2b cDNA (clone 5ERB14, provided by Dr. John A. Payne) (17) that was predigested with SpeI and MunI. Finally, the full-length KCC2a and KCC2b cDNAs were ligated into the XbaI and HindIII sites of the pcDNA3.1 expression vector (Invitrogen).

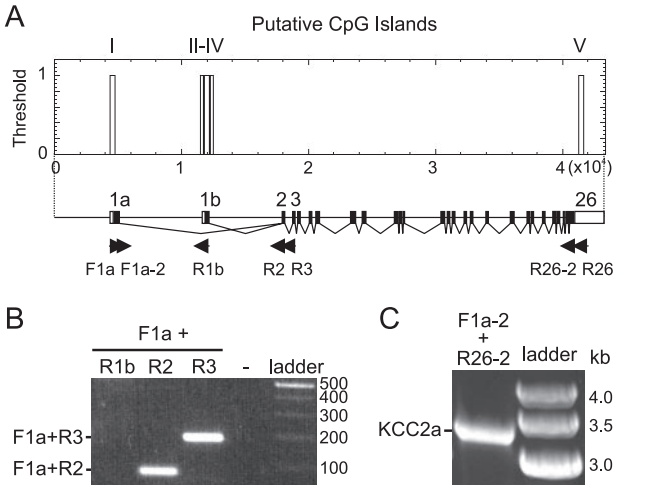

FIGURE 1. **Identification of a new upstream exon-1a in the KCC2 gene.** *A*, five putative CpG islands (*I–V*) were predicted (see "Experimental Procedures") within a 40-kb genomic fragment that includes the KCC2 gene and flanking regions. The KCC2 gene (official name *SLC12A5*) consists of 26 exons in mammals (34). CpG islands II-IV are located in the previously characterized KCC2 promoter and 5′-UTR region (19), and CpG island V is situated in the 3′-UTR region of the KCC2 gene. CpG island I corresponds to the promoter and 5′-UTR of a novel KCC2 exon (exon-1a) based on a match to two human expressed sequence tags that extend to KCC2 exon-2 (and downstream exons). The KCC2 gene structure and positions of primers used in subsequent experiments appear below. *B*, RT-PCR analysis of an adult mouse cortex (see "Experimental Procedures") detected a direct splicing of the new exon-1a to exon-2. *C*, expression of a full-length KCC2a in a rat brain. First-strand cDNA was synthesized using a KCC2 3′-UTR-specific primer, R26 (supplemental Table S1) and used in a PCR with the R26- and exon-1a-specific F1a primers. An aliquot of this reaction was further amplified in a nested PCR with F1a-2 and R26-2 primers that produced a single DNA band of expected size.

RESULTS

Identification of a New Upstream Exon in the KCC2 Gene—We have recently characterized the promoter responsible for the transcription of the previously known neuron-specific and developmentally up-regulated KCC2 isoform (17, 19, 20). Tran-

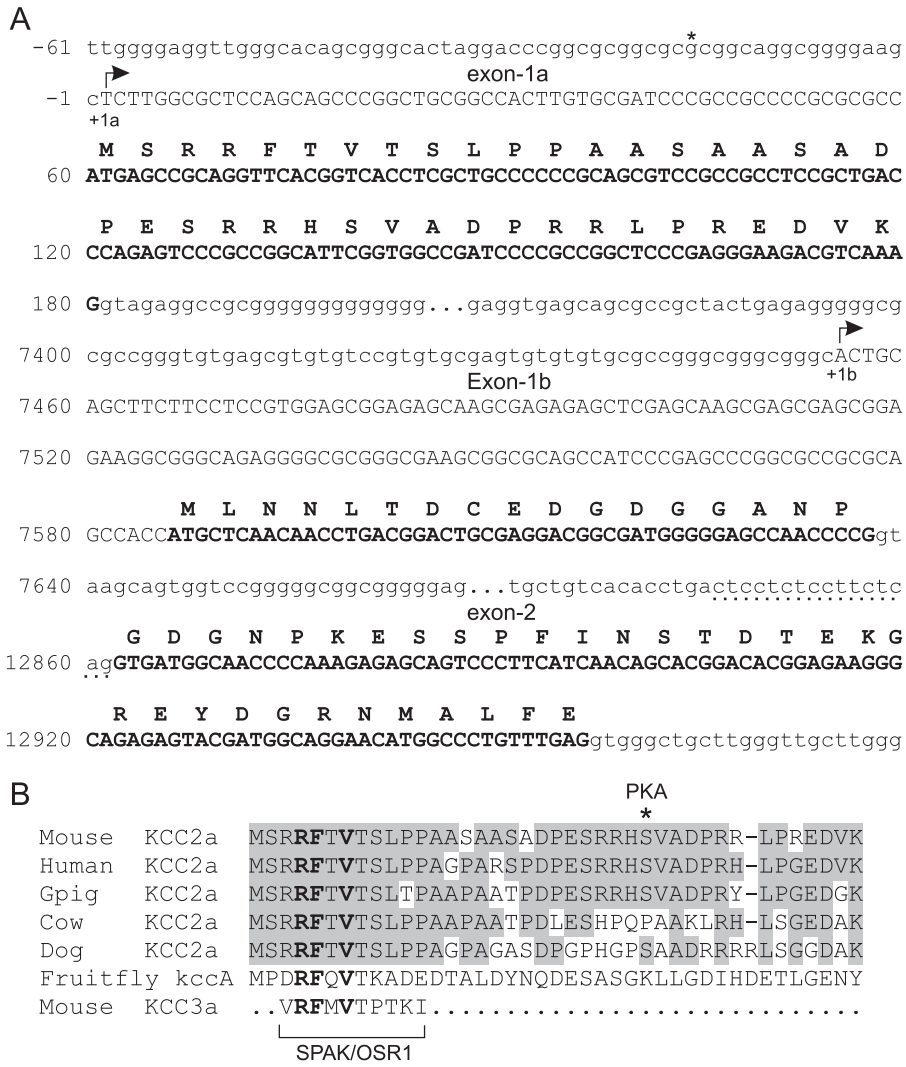

FIGURE 2. **Alternatively spliced KCC2a and KCC2b isoforms have different N-terminal parts.** *A*, the genomic sequence of the mouse KCC2 gene from exon-1a up to exon-2 is shown. Introns are presented in *lowercase letters*, exons appear in *capital letters*, and the coding parts of exons are highlighted in *bold*. The amino acid sequences are shown above the corresponding nucleotide sequences. Note a classical splice acceptor site with pyrimidine tract (*dotted line*) upstream of exon-2 that is consistent with the effective splicing of exon-1a (and exon-1b) to exon-2. Transcription start sites are marked with *arrows*. The expressed sequence tag clone farthest upstream that is homologous to the KCC2a sequence stops at position −17 bp (marked with an *asterisk*) relative to the exon-1a transcription start site obtained via 5′-RACE. *B*, alignment of KCC2a N-terminal sequences from selected mammals. The guinea pig (*gpig*), cow, and dog sequences were predicted from the corresponding genome data bases using the mouse KCC2a N terminus sequence as a query. Note the conservation of the N-terminal part that includes critical residues for the putative SPAK/OSR1 binding site (marked in *bold*). The N terminus of Drosophila kcc splice forms A/D and the proposed SPAK/OSR1 binding site in mouse KCC3a appear for comparison. Ser-27, predicted to be a substrate for protein kinase A (*PKA*) phosphorylation in the mouse sequence, is marked with an *asterisk*.

scription start sites are often associated with CpG islands (21). To identify possible new alternative promoters for KCC2, we analyzed a ~40-kb human genomic fragment bearing the KCC2 gene using a CpG island-finding tool. This predicted several CpG islands within the previously characterized KCC2 promoter region but also one CpG island ~7 kb upstream of the known KCC2 promoter (Fig. 1*A*) that was a candidate for an alternative KCC2 promoter.

A BLAST search using the upstream CpG island sequence as a query revealed two human expressed sequence tag clones (DA102113 and DA328785) matching a putative novel KCC2 exon (named exon-1a) spliced directly to exon-2 and subsequent KCC2 exons (up to exon-5). This suggested the existence of an alternative KCC2 transcript starting from the novel exon-1a. The genomic sequence corresponding to the KCC2 exon-1a is highly conserved between human, mouse, and rat genomes. A few expressed sequence tags homologous to the human KCC2 exon-1a sequence were found in the mouse but they were not spliced directly to KCC2 exon-2 (data not shown). To address whether a corresponding alternative KCC2 transcript starting from exon-1a is expressed in mice, we assayed adult mouse brain samples by RT-PCR using different combinations of KCC2 forward and reverse primers (Fig. 1, *A* and *B*, and supplemental Table S1). A PCR product of the predicted size (~100 bp) was amplified with exon-1a forward (*F1a*) and exon-2 reverse (*R2*) primers, suggesting that these two exons were spliced directly. This result was confirmed using the F1a forward and exon-3, exon-5, or exon-7 reverse primers (Fig. 1*B* and data not shown). Sequencing of these PCR fragments revealed no insertions between exon-1a and exon-2.

To demonstrate that a full-length KCC2 isoform containing exon-1a (KCC2a) is expressed *in vivo*, we carried out nested RT-PCR from total RNA isolated from an embryonic day E18 rat hippocampus. This resulted in a PCR product of expected size ~3.4 kb (Fig. 1*C*), and its sequencing confirmed that KCC2a mRNA differs from KCC2b transcript only by the presence of exon-1a instead of exon-1b, so that all the other KCC2 exons (from exon-2 to exon-26) are identical in both isoforms.

Exon-1a Encodes a Novel N Terminus That Includes a Putative SPAK/OSR1 Binding Motif—To identify the transcription start site(s) and the initiation methionine for the KCC2a isoform, we performed 5′-rapid amplification of cDNA ends (5′-RACE). Analysis of the longest PCR product obtained indicates that the novel KCC2 exon-1a comprises a 5′-UTR of at least 59 bp followed by the initiation methionine and 121 bp encoding 40 amino acids that are specific for KCC2a (Fig. 2*A*).

Residues 3–12 in the KCC2 exon-1a are highly conserved among mammals and comprise a sequence similar to the Ste20-related proline alanine-rich kinase/oxidative stress response-1

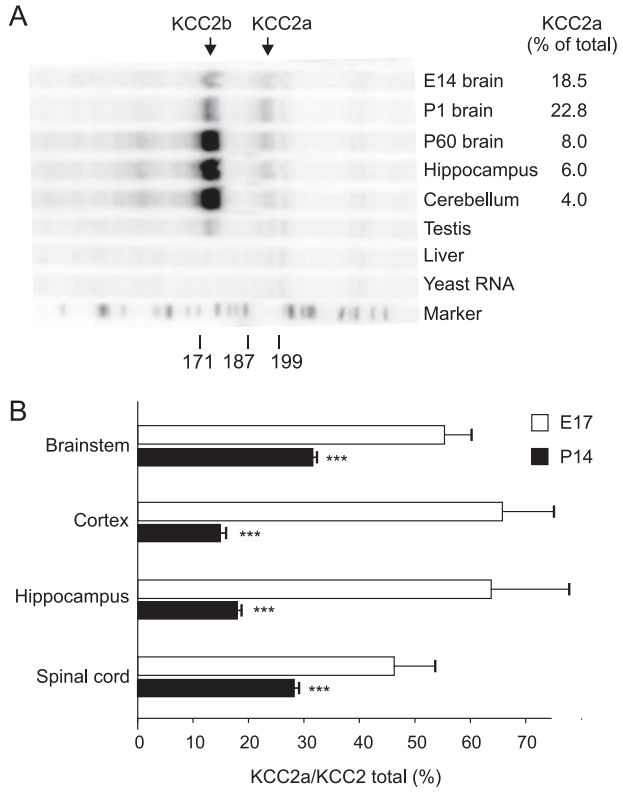

FIGURE 3. **KCC2a contributes 20–50% of total KCC2 expression in the embryonic and early postnatal brain.** *A*, RNA protection assay using a probe that spans exon-1a to exon-3 (see "Experimental Procedures") results in an 18-bp difference in the length of the protected fragments corresponding to KCC2a and KCC2b mRNAs. Both KCC2a and KCC2b mRNAs are expressed in the mouse brain, but not in the liver. The weak signal in the testis presumably represents aberrant low level expression of a truncated transcript (35). In contrast to the significantly increased expression of KCC2b during mouse brain development, the KCC2a expression remains relatively constant. KCC2a expression constituted ~23% of total KCC2 expression in the whole brain at postnatal day 1, but only ~8% at day 60. *B*, real-time PCR quantification of KCC2a and KCC2b mRNA levels in different brain regions (see "Experimental Procedures") indicates that the levels do not differ significantly at embryonic day E17, whereas KCC2b is several times more abundant than KCC2a at postnatal day P14. Values are mean ± S.E. of three independent experiments. ***, $p < 0.001$ between the KCC2a and KCC2b levels by *t* test.

(SPAK/OSR1) binding motif (22) (Fig. 2*B*). In addition, several putative Ser and Thr phosphorylation sites were predicted within the 40 residues encoded by exon-1a (Fig. 2*B* and data not shown). One of these sites, Ser-27, had the highest score among all predicted Ser/Thr phosphorylation sites within the 1139-residue-long mouse KCC2a isoform. Protein kinase A was predicted to be the most probable kinase for phosphorylation of Ser-27.

KCC2a and KCC2b mRNA Levels Are Not Significantly Different in Newborn Mouse Brain, but KCC2b Expression Is Steeply Up-regulated during Postnatal Development—To study the expression pattern of KCC2a and to evaluate the relative expression of KCC2a and KCC2b mRNAs, we carried out an RPA using total RNA isolated from multiple mouse tissues with a probe that simultaneously detects the KCC2a and KCC2b isoforms. RPA showed expression of both KCC2 isoforms in the brain, whereas no specific signal was observed in the liver (Fig. 3*A*). The level of KCC2a mRNA was lower in the adult brain than that of KCC2b and consisted of only 4–8% of total KCC2 (KCC2a + KCC2b) mRNA (Fig. 3*A*). In contrast, the relative expression of KCC2a mRNA was clearly higher (~19–23% of total KCC2 mRNA expression) in the embryonic and neonatal brain (Fig. 3*A*).

To further compare the relative expression of KCC2a *versus* KCC2b mRNAs in different CNS regions and at different developmental stages, we used quantitative (real-time) RT-PCR (Fig. 3*B*). Because exon-1b mRNA tends to form strong hairpin structures that prevent effective cDNA synthesis (supplemental Fig. S1 and data not shown), first-strand cDNA synthesis was accomplished with KCC2 exon-2-specific primer R2, which allowed cDNA synthesis at high temperature. Under these conditions, the relative expression of KCC2a and KCC2 mRNAs were similar at embryonic day E17 in all the brain regions examined (Fig. 3*B*). The situation was clearly different at postnatal day P14: KCC2a expression was three to six times lower than that of KCC2b, ranging from ~32% of total KCC2 expression in the brain stem to ~13% in the cerebellum (Fig. 3*B* and data not shown). Taken together, the RPA and quantitative RT-PCR results indicate that the two KCC2 isoforms are expressed at nearly comparable levels in the prenatal and early postnatal brain but KCC2b mRNA expression level was clearly higher than that of KCC2a during late postnatal development.

KCC2a mRNA Expression Is Restricted to the Central Nervous System and Is Not Significantly Up-regulated during Postnatal Development—Previous studies of KCC2 expression have used PCR primers, *in situ* probes, or antibodies that detect both KCC2 isoforms (1, 5–7, 17, 23). We compared the temporal and regional expression of KCC2a and KCC2b mRNA in a mouse brain by *in situ* hybridization using probes specific for each isoform. Hybridization of adult mouse brain sections with an exon-1b-specific probe revealed an expression pattern similar to that obtained with long probes detecting both KCC2 isoforms (supplemental Fig. S2; compare with Refs. 17 and 23). However, the probe, being GC-rich (>70%) and relatively short (~100 bp), produced a high background and failed to detect KCC2b mRNA in embryonic and early postnatal brains. The same problem (>75% GC-rich and short length of the exon-1a probe) coupled with the lower expression of KCC2a in the adult brain (Fig. 3*A*) hindered the detection of KCC2a mRNA by *in situ* hybridization (data not shown).

Thus, to compare KCC2a mRNA expression between different CNS regions and at different time points, we performed RT-PCR using random primers in first-strand cDNA synthesis to allow GAPDH normalization. First, to confirm the absence of KCC2a mRNA in non-neuronal tissues, and to obtain a qualitative estimate of KCC2a and KCC2b expression in different CNS areas, the cDNA was subjected to 40 cycles of amplification in a conventional PCR with KCC2a-, KCC2b-, and GAPDH-specific primers. In E17 mouse embryos, KCC2a expression was clearly detected in the brain stem, spinal cord, and olfactory bulb, while PCR signals were very low in the cortex and hippocampus (Fig. 4*A*). PCR with KCC2b primers showed a similar expression pattern. Neither KCC2a nor KCC2b was detected in any non-neuronal tissues examined. Likewise, both KCC2 isoforms were present in all brain regions analyzed, but not in non-neuronal tissues at P14 (Fig. 4*B*).

Quantitative RT-PCR indicated that KCC2a mRNA levels (relative to GAPDH levels) in E17 mouse brain stem were ~5-fold higher than in the cortex (Fig. 4*C*), which is consistent with the results of the qualitative PCR (Fig. 4*A*). In contrast,

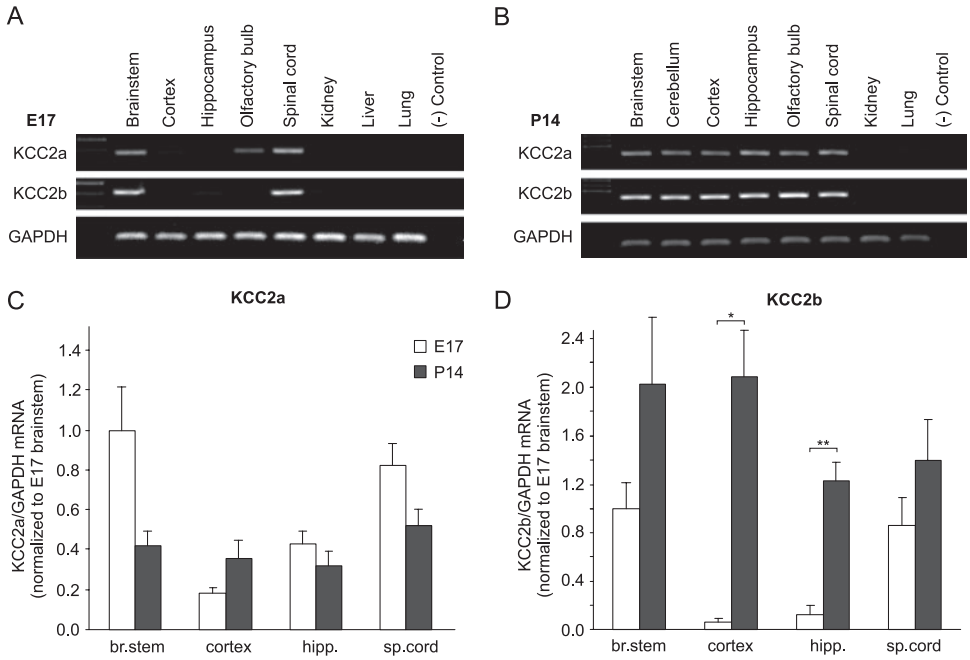

FIGURE 4. **KCC2a mRNA expression is restricted to CNS and remains relatively constant during postnatal development.** *A* and *B*, semiquantitative RT-PCR analysis of KCC2a and KCC2b mRNA expression in different brain regions and non-neuronal tissues from E17 (*A*) and P14 (*B*) mice. *C* and *D*, quantitative real-time PCR analysis of KCC2a (*C*) and KCC2b (*D*) mRNA expression relative to GAPDH in different brain regions of E17 and P14 mice (see "Experimental Procedures"). The values are normalized to E17 brain stem levels. At E17, both KCC2a and KCC2b mRNA expression is higher in the brain stem than in the cortex. Although relative KCC2b mRNA levels increased dramatically in the neocortex and hippocampus between E17 and P14, relative KCC2a mRNA levels did not change significantly. Values are mean ± S.E. of three experiments. *, $p < 0.05$; **, $p < 0.01$ by *t* test.

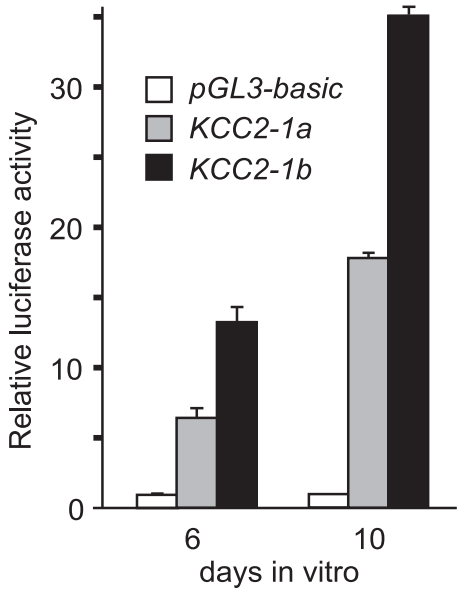

FIGURE 5. **KCC2a promoter is active in primary neurons.** Dissociated cortical neuronal cultures (2×10^5 cells/cm^2) were prepared from E18 rat embryos as described previously (20). After 4 or 8 days *in vitro*, the neurons were cotransfected with the KCC2-1b, KCC2-1a, or pGL3-Basic firefly luciferase constructs simultaneously with the *Renilla* luciferase pRL-TK construct and analyzed 48 h later. Values are mean ± S.E. of three independent experiments.

different CNS areas expressed comparable levels of KCC2a mRNA at P14 (Fig. 4*C*). KCC2b expression at E17 was 10–15 times lower in the hippocampus and cortex than in the brain stem. In contrast to KCC2a, the expression of KCC2b increased strongly in the hippocampus (~10-fold) and neocortex (~35-fold) (Fig. 4*D*).

KCC2a Promoter Is Active in Neurons—To establish that the genomic region upstream of exon-1a possesses transcription activity in cultured neurons, we cloned ~1 kb of mouse genomic sequence upstream of the predicted KCC2a transcription start site (Fig. 2*A*) into a promoterless luciferase reporter vector. The luciferase activity of this reporter (named *KCC2-1a*) was compared with that of the previously characterized 1.4-kb KCC2b promoter (*KCC2-1b*) (19). Both constructs produced robust luciferase activity in DIV5 and DIV10 cultured rat cortical neurons, although the activity of *KCC2-1b* was ~2-fold higher (Fig. 5). This result indicated that the KCC2a proximal promoter is active in primary neurons.

KCC2a Can Mediate ^{86}Rb Transport in HEK293 Cells—To address whether the KCC2a isoform is able to mediate K-Cl cotransporter activity in mammalian cells, we performed functional ^{86}Rb uptake assays in HEK293 cells (18). Western blot analysis demonstrated that both isoforms were strongly expressed in HEK293 cells transiently transfected with the KCC2a (KCC2a-HEK293) and KCC2b (KCC2b-HEK293) constructs (supplemental Fig. S3). Upon transfection, ^{86}Rb uptake increased 2.5-fold in KCC2a-HEK293 and 2.4-fold in KCC2b-HEK293 compared with non-transfected HEK293 cells (Fig. 6). After pretreatment with furosemide (2 mM), a known inhibitor of K-Cl cotransporters, the remaining ^{86}Rb influx in the KCC2a- and KCC2b-transfected cells was similar to that in non-transfected cells (Fig. 6). These results indicate that KCC2a is active in HEK293 cells without exogenous stimulation, similar to KCC2b isoform reported previously (18). The application of NEM (1 mM), a sulfydryl alkylating agent widely used to activate K-Cl cotransporters (24), increased ^{86}Rb uptake 2.2-fold in the KCC2a- and 1.6-fold in the KCC2b-transfected cells but not in the non-transfected ones (Fig. 6). The NEM-induced activation of ^{86}Rb uptake in the KCC2a- and KCC2b-transfected cells was completely blocked by furosemide (Fig. 6). Thus, NEM increased the furosemide-sensitive ^{86}Rb uptake 2.6-fold in the KCC2a-HEK293 and 1.7-fold in the KCC2b-HEK293 cells (Fig. 6). Together, the results indicate that KCC2a can mediate isotonic ^{86}Rb uptake comparable with that of KCC2b in mammalian cells.

KCC2b-deficient Mice Retain KCC2a mRNA Expression—KCC2 null mutant mice, produced by the deletion of exon-5 (3) or disruption of exon-4 (25), both of which result in a complete lack of KCC2 protein, die at birth due to severe motor deficits, including respiration failure. In contrast, the targeted disruption of KCC2 exon-1b produced mice that can survive for 2 weeks after birth (14). Because these mice retain 5–8% of normal KCC2 protein levels (at postnatal day P10–12), and exon-1a

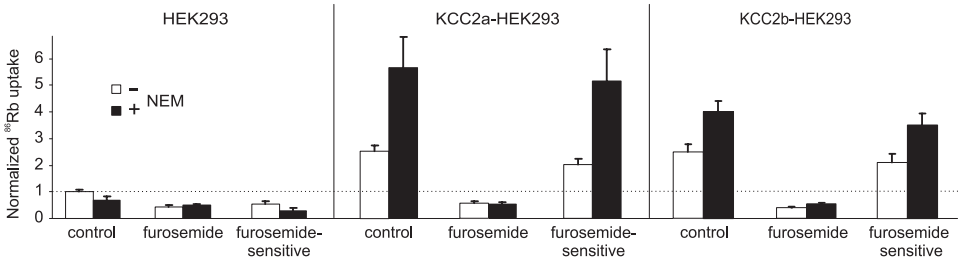

FIGURE 6. **KCC2a and KCC2b can mediate comparable furosemide-sensitive and NEM-induced ^{86}Rb influx in HEK293 cells.** ^{86}Rb uptake in HEK293 cells transiently transfected by KCC2a or KCC2b expression constructs was significantly higher than in non-transfected cells. Furosemide (2 mM) strongly inhibited, whereas *N*-ethylmaleimide (*NEM*) (1 mM) significantly increased ^{86}Rb uptake in KCC2a- and KCC2b-transfected cells. The NEM-induced activation of ^{86}Rb uptake was completely blocked by furosemide. Furosemide-sensitive ^{86}Rb uptake was 2.5-fold higher in KCC2a-HEK293 and 2.4-fold higher in KCC2b-HEK293 cells than in non-transfected HEK293 cells. Transfection efficiency in the experiments was ~50% (based on transfecting the parallel HEK293 cultures with a green fluorescent protein construct). NEM increased the furosemide-sensitive ^{86}Rb uptake by 2.6-fold in KCC2a- and 1.7-fold in KCC2b-expressing cells but slightly decreased ^{86}Rb uptake in non-transfected HEK293 cells. Values are the mean ± S.E. of four experiments.

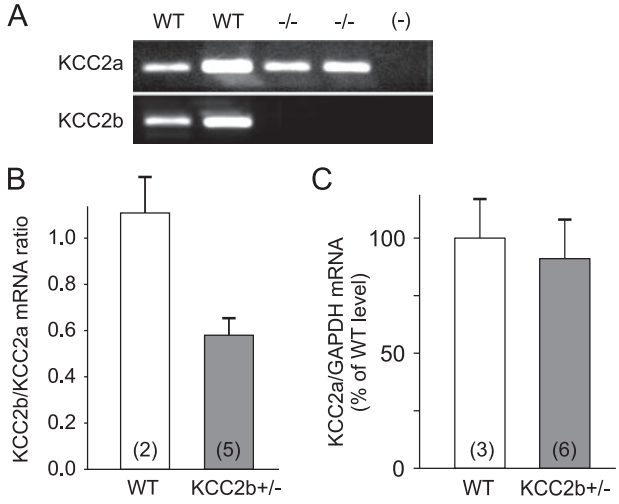

FIGURE 7. **KCC2 exon-1b-targeted mice lack KCC2b but retain normal KCC2a mRNA expression.** *A*, RT-PCR analysis (see "Experimental Procedures") showing that mice homozygous (−/−) for the KCC2 exon-1b disruption (14) lack KCC2b but express KCC2a mRNA in the brain. *B*, real-time PCR quantification of KCC2a mRNA relative to KCC2b mRNA levels in P3 littermate mouse brains that were wild-type (*WT*) or heterozygous (+/−) for the KCC2 exon-1b disruption. *C*, KCC2a mRNA expression relative to GAPDH is not different between the genotypes. The number of mice in each group is indicated in *parentheses*.

remains intact in these mice, we assumed that the remaining KCC2 would be attributed to the KCC2a isoform. To confirm this, we used RT-PCR to compare the expression of KCC2a and KCC2b mRNAs in the brains of littermate mice that were wild-type, heterozygous (KCC2b$^{+/-}$), or homozygous (KCC2b$^{-/-}$) for the KCC2 exon-1b disruption. As expected, KCC2b mRNA expression was absent in brains from homozygous KCC2b$^{-/-}$ mice, while KCC2a mRNA was present (Fig. 7*A*). Consistent with the presence of only one functional KCC2b allele in the heterozygous KCC2b$^{+/-}$ mice, the proportion of KCC2b to KCC2a mRNA in the KCC2b$^{+/-}$ mouse brain was ~50% lower than in their wild-type littermates (Fig. 7*B*). In contrast, KCC2a expression (relative to GAPDH) remained unchanged between the genotypes (Fig. 7*C*).

DISCUSSION

Here we have characterized a novel neuron-specific KCC2a isoform produced by an alternative promoter and first exon usage. The KCC2a isoform differs from the previously known major KCC2b isoform by 40 unique N-terminal amino acid residues that comprise a putative SPAK/OSR1 binding motif. Although the postnatal increase in the major KCC2b isoform prevails over that of KCC2a in the cortex during late postnatal development, the KCC2a and KCC2b isoforms show nearly comparable mRNA levels in the brain stem and spinal cord during prenatal and early postnatal stages. This suggests that KCC2a may play an important role in the developing brain stem and spinal cord.

Consistent with this idea, mice that lack KCC2b but retain an apparently normal level of KCC2a expression survive for up to 2 weeks (14), whereas mice lacking both KCC2 isoforms die immediately after birth due to severe motor defects, including respiration failure (3, 25). The amount of KCC2 protein remaining in the KCC2b-deficient mouse brain correlates with the KCC2a mRNA levels. However, a detailed comparison of KCC2a mRNA and protein levels in different brain areas and at developmental time points remains a subject of future studies. Nevertheless, we suggest that KCC2a expression is sufficient to reduce intracellular chloride to a level necessary to maintain basic inhibitory functions such as the motor control of respiration, required for survival. Because the KCC2b-deficient mice eventually die of spontaneous seizures by the end of the second postnatal week, KCC2a levels in the cortex are presumably too low to support the higher chloride extrusion efficiency required for hyperpolarizing inhibition in mature cortical neuronal networks.

In agreement with the previous data showing that KCC2 is exclusively expressed in CNS neurons, both KCC2a and KCC2b mRNAs were undetectable by RT-PCR in all peripheral tissues examined. The lack of KCC2 in CNS glial cells in previous studies using C-terminal antibodies and 3′ *in situ* hybridization probes that detect both KCC2 isoforms suggests that both KCC2 isoforms are restricted to CNS neurons. Consistent with this, the distribution pattern of the weak KCC2 immunoreactivity that remains in the brain stem of mice lacking KCC2b (26) resembles the pattern of KCC2 immunoreactivity in wild-type mice. Additional studies using KCC2b-deficient mice should confirm this and address whether the subcellular distribution of the two KCC2 isoforms is similar. Together the results indicate that both KCC2a and KCC2b isoforms are restricted to CNS neurons, although the regulation of their expression clearly differs during cortical development.

Regulatory elements within the KCC2b promoter region, including binding sites for neuron-enriched transcription factors such as Egr4, seem largely sufficient to drive the neuron-specific expression of KCC2b mRNA, whereas the neuronal restrictive silencing element located in the intron-1b of the KCC2 gene (27) is dispensable (19, 20). The predicted ~430-bp proximal KCC2a promoter contains a putative TATA box and conserved binding

sites for ubiquitous transcription factors (such as E2F and HNF4) but no obvious conserved sites for neuron-enriched transcription factors (data not shown). Thus, the mechanisms that restrict the expression of KCC2a to CNS neurons remain to be studied. The neuronal restrictive silencing element in intron-1b and/or another neuronal restrictive silencing element located in intron-7 of the KCC2 gene (28, 29) may contribute to this restriction.

Of the four K-Cl cotransporters (KCC1-KCC4), KCC2 is unique in mediating constitutive K-Cl cotransport under isotonic conditions because of a distinct C-terminal domain (30). Consistent with this, functional ^{86}Rb uptake assays in HEK293 cells indicated that both KCC2 isoforms can mediate robust ion transport activity without exogenous stimulation. The furosemide-sensitive ^{86}Rb uptake in HEK293 cells transiently transfected with KCC2a or KCC2b was similar in magnitude to that reported in stably transfected KCC2b-HEK293 cells (18). Furthermore, induction of the furosemide-sensitive ^{86}Rb uptake by NEM was comparable between the two KCC2 isoforms in the transiently transfected HEK293 cells and similar in magnitude to that previously observed (23).

Several Ser/Thr residues within exon-1a were predicted to be phosphorylation sites and thus candidates to regulate the function of the KCC2a isoform. However, none of them was completely conserved among different mammals. In contrast, the most N-terminal part of the exon that comprises a putative SPAK binding sequence was highly conserved among mammals. Although the sequence in KCC2a differs slightly (R against G/V/S in position −1 and L against S/T/V/I in +7 position) from the published SPAK binding consensus motif (21), the critical 1st, 2nd, and 4th positions are present (31). A recent study reported a putative Drosophila fly KCC2 homolog kazachoc (*kcc*) that also generates alternative splice forms with different N termini: one is enriched in adult neurons and the other, in embryos (32). Interestingly, the three critical residues of the proposed SPAK/OSR1 kinase binding site also appear in the N terminus of the embryonic *kcc* splice form (Fig. 2*B*). Even if KCC2b does not have a SPAK binding motif, SPAK can regulate KCC2b function in *Xenopus laevis* oocytes (33). It will be interesting to study whether SPAK binds and regulates the activities of the KCC2 isoforms differently.

Acknowledgments—We thank Matt Phillips for help in bioinformatics, Seija Lehto and Outi Nikkilä for the neuronal cultures, and Marjo Heikura and Miika Palviainen for the in situ hybridization.

REFERENCES

1. Rivera, C., Voipio, J., Payne, J. A., Ruusuvuori, E., Lahtinen, H., Lamsa, K., Pirvola, U., Saarma, M., and Kaila, K. (1999) *Nature* **397,** 251–255
2. Payne, J. A., Rivera, C., Voipio, J., and Kaila, K. (2003) *Trends Neurosci.* **26,** 199–206
3. Hubner, C. A., Stein, V., Hermans-Borgmeyer, I., Meyer, T., Ballanyi, K., and Jentsch, T. J. (2001) *Neuron* **30,** 515–524
4. Mercado, A., Mount, D. B., and Gamba, G. (2004) *Neurochem. Res.* **29,** 17–25
5. Lu, J., Karadsheh, M., and Delpire, E. (1999) *J. Neurobiol.* **39,** 558–568
6. Li, H., Tornberg, J., Kaila, K., Airaksinen, M. S., and Rivera, C. (2002) *Eur. J. Neurosci.* **16,** 2358–2370
7. Stein, V., Hermans-Borgmeyer, I., Jentsch, T. J., and Hubner, C. A. (2004) *J. Comp. Neurol.* **468,** 57–64
8. Kimura, K., Wakamatsu, A., Suzuki, Y., Ota, T., Nishikawa, T., Yamashita, R., Yamamoto, J., Sekine, M., Tsuritani, K., Wakaguri, H., Ishii, S., Sugiyama, T., Saito, K., Isono, Y., Irie, R., Kushida, N., Yoneyama, T., Otsuka, R., Kanda, K., Yokoi, T., Kondo, H., Wagatsuma, M., Murakawa, K., Ishida, S., Ishibashi, T., Takahashi-Fujii, A., Tanase, T., Nagai, K., Kikuchi, H., Nakai, K., Isogai, T., and Sugano, S. (2006) *Genome Res.* **16,** 55–65
9. Landry, J. R., Mager, D. L., and Wilhelm, B. T. (2003) *Trends Genet.* **19,** 640–648
10. Adragna, N. C., Fulvio, M. D., and Lauf, P. K. (2004) *J. Membr. Biol.* **201,** 109–137
11. Mercado, A., Vazquez, N., Song, L., Cortes, R., Enck, A. H., Welch, R., Delpire, E., Gamba, G., and Mount, D. B. (2005) *Am. J. Physiol.* **289,** F1246–F1261
12. Le Rouzic, P., Ivanov, T. R., Stanley, P. J., Baudoin, F. M., Chan, F., Pinteaux, E., Brown, P. D., and Luckman, S. M. (2006) *Brain Res.* **1110,** 39–45
13. Di Fulvio, M., Lauf, P. K., and Adragna, N. C. (2003) *Nitric Oxide* **9,** 165–171
14. Woo, N. S., Lu, J., England, R., McClellan, R., Dufour, S., Mount, D. B., Deutch, A. Y., Lovinger, D. M., and Delpire, E. (2002) *Hippocampus* **12,** 258–268
15. Obenauer, J. C., Cantley, L. C., and Yaffe, M. B. (2003) *Nucleic Acids Res.* **31,** 3635–3641
16. Timmusk, T., Belluardo, N., Metsis, M., and Persson, H. (1993) *Eur. J. Neurosci.* **5,** 605–613
17. Payne, J. A., Stevenson, T. J., and Donaldson, L. F. (1996) *J. Biol. Chem.* **271,** 16245–16252
18. Payne, J. A. (1997) *Am. J. Physiol.* **273,** C1516–C1525
19. Uvarov, P., Pruunsild, P., Timmusk, T., and Airaksinen, M. S. (2005) *J. Neurochem.* **95,** 1144–1155
20. Uvarov, P., Ludwig, A., Markkanen, M., Rivera, C., and Airaksinen, M. S. (2006) *J. Neurosci.* **26,** 13463–13473
21. Larsen, F., Gundersen, G., Lopez, R., and Prydz, H. (1992) *Genomics* **13,** 1095–1107
22. Delpire, E., and Gagnon, K. B. (2007) *Physiol. Genomics* **28,** 223–231
23. Kanaka, C., Ohno, K., Okabe, A., Kuriyama, K., Itoh, T., Fukuda, A., and Sato, K. (2001) *Neuroscience* **104,** 933–946
24. Gillen, C. M., Brill, S., Payne, J. A., and Forbush, B., III (1996) *J. Biol. Chem.* **271,** 16237–16244
25. Tornberg, J., Voikar, V., Savilahti, H., Rauvala, H., and Airaksinen, M. S. (2005) *Eur. J. Neurosci.* **21,** 1327–1337
26. Blaesse, P., Guillemin, I., Schindler, J., Schweizer, M., Delpire, E., Khiroug, L., Friauf, E., and Nothwang, H. G. (2006) *J. Neurosci.* **26,** 10407–10419
27. Karadsheh, M. F., and Delpire, E. (2001) *J. Neurophysiol.* **85,** 995–997
28. Bruce, A. W., Donaldson, I. J., Wood, I. C., Yerbury, S. A., Sadowski, M. I., Chapman, M., Gottgens, B., and Buckley, N. J. (2004) *Proc. Natl. Acad. Sci. U. S. A.* **101,** 10458–10463
29. Wu, J., and Xie, X. (2006) *Genome Biol.* **7,** R85
30. Mercado, A., Broumand, V., Zandi-Nejad, K., Enck, A. H., and Mount, D. B. (2006) *J. Biol. Chem.* **281,** 1016–1026
31. Piechotta, K., Lu, J., and Delpire, E. (2002) *J. Biol. Chem.* **277,** 50812–50819
32. Hekmat-Scafe, D. S., Lundy, M. Y., Ranga, R., and Tanouye, M. A. (2006) *J. Neurosci.* **26,** 8943–8954
33. Gagnon, K. B., England, R., and Delpire, E. (2006) *Am. J. Physiol.* **290,** C134–C142
34. Song, L., Mercado, A., Vazquez, N., Xie, Q., Desai, R., George, A. L., Jr., Gamba, G., and Mount, D. B. (2002) *Brain Res. Mol. Brain Res.* **103,** 91–105
35. Williams, J. R., Sharp, J. W., Kumari, V. G., Wilson, M., and Payne, J. (1999) *J. Biol. Chem.* **274,** 12656–12664